Bioorganic & Medicinal Chemistry 20 (2012) 5699–5704

Contents lists available at SciVerse ScienceDirect

Bioorganic & Medicinal Chemistry

journal homepage: www.elsevier.com/locate/bmc

Possible conformation of amphotericin B dimer in membrane-bound assembly as deduced from solid-state NMR

Yuichi Umegawa, Takeshi Adachi, Nobuaki Matsumori *, Michio Murata *

Department of Chemistry, Graduate School of Science, Osaka University, 1-1 Machikaneyama, Toyonaka, Osaka 560-0043, Japan

ARTICLE INFO

Article history:
Available online 19 August 2012

Keywords:
Amphotericin B
Dimer
Ion channel
Solid-state NMR
Rotational echo double resonance

ABSTRACT

Aiming for structural analysis of amphotericin B (AmB) ion-channel assemblies in membrane, a covalent dimer was synthesized between ^{13}C-labled AmB methyl ester and ^{19}F-labled AmB. The dimer showed slightly weaker but significant biological activities against fungi and red blood cells compared with those of monomeric AmB. Then the dimer was subjected to ^{13}C{^{19}F}REDOR (Rotational-Echo Double Resonance) experiments in hydrated lipid bilayers. The obtained REDOR dephasing effects were explained by two components; a short ^{13}C/^{19}F distance (6.9 Å) accounting for 23% of the REDOR dephasing, and a longer one (14 Å) comprising the rest of the dephasing. The shorter distance is likely to reflect the formation of barrel-stave ion channel.

1. Introduction

Amphotericin B (AmB) is one of the standard anti-fungal drug used for treatment of deep-seated fungal infections despite its serious side effects.[1,2] It is widely accepted that the mechanism of action of AmB is responsible for the formation of a 'barrel-stave' self-assembly that is thought to act as an ion permeable channel in fungal cell membrane.[3,4] Its selective toxicity has been accounted for by intermolecular AmB-sterol recognition; AmB prefers to ergosterol, a major sterol in fungal membrane, than cholesterol in mammalian membrane.[5,6] From the clinical, biophysical and biochemical significance, the AmB channel structure has been investigated by computational simulations[7–9] and spectroscopic methods[10–12] including solid-state NMR.[13,14]

On the other hand, recent studies based on chemical synthesis have suggested a new possible mechanism for anti-fungal activity[15]; for example, Burke's group synthesized 41-methyl AmB[16] and 35-deoxy AmB,[17] and found that both derivatives retained anti-fungal activity, although the latter was devoid of membrane-permeabilizing effects against artificial liposomes. From these findings, they proposed a new mechanism for antifungal action of AmB; the drug exerts antifungal activity by simply binding and trapping the ergosterol molecules rather than by forming an ion channel, and membrane permeabilization via channel formation represents a second complementary mechanism that further increases drug potency and the rate of yeast killing. Nevertheless, the structure of ion channel complex itself is crucial to provide information as to whether or not the channel formation is primarily related to the biological activity.

During the last several years, we have attempted to elucidate the structure of AmB ion channel using various approaches. To examine the AmB-ergosterol binding structure, we previously prepared a series of derivatives whose mycosamine orientation was restricted by covalent linkage between the amino and carbonyl groups, and suggested that the orientation of mycosamine crucially affected the sterol selectivity and ion channel formation.[18] Baginski's group also reported using computational calculations that conformation of a mycosamine moiety is changed by binding to ergosterol.[19] More recently, Carreira's group derivatized the sugar moiety of AmB,[20] and found that 2′-OH is essential for the interaction with an ergosterol molecule.

In addition to derivatization of AmB, we have also used solid-state NMR techniques including ^{2}H and ^{19}F resonances to observe molecular orientation and mobility in hydrated lipid bilayers.[21,22] Among other solid-state NMR methods, rotational echo double resonance (REDOR),[23,24] a triple resonance method for measuring interatomic distance, turned out to be particularly useful for elucidating the structure of membrane-bound molecular assemblies. Using this technique, we estimated the intermolecular distances between AmB–AmB and AmB-ergosterol.[25–27]

Toward the analysis of binary interactions between AmB molecules in detail, we have also synthesized several AmB covalent dimers in order to stabilize the complexed state in membrane for a longer period enough for solid state NMR measurements. We first prepared various dimers cross-linked between the amino groups (N–N dimers)[28,29] and between the carbonyl groups (C–C dimers),[30] and both N–N and C–C dimers revealed significant membrane permeabilizing activity. In particular, an N–N dimer with a tartrate

* Corresponding authors.
E-mail addresses: matsmori@chem.sci.osaka-u.ac.jp (N. Matsumori), murata@chem.sci.osaka-u.ac.jp (M. Murata).

0968-0896/$ - see front matter © 2012 Elsevier Ltd. All rights reserved.
http://dx.doi.org/10.1016/j.bmc.2012.08.016

linkage between amino groups revealed potent hemolytic activity as compared with that of monomeric AmB.[29] More recently, we have recorded a single channel current of the tertrate N–N dimer, and proposed a new AmB channel model, comprising of six monomeric AmB molecules.[31] We also synthesized AmB dimers with a linkage between the amino and carbonyl groups (C–N dimers)[32] to mimic the proposed intermolecular interaction between AmBs,[11] and found that a C–N dimer with a relatively long linker (dimer **4**, Fig. 1) retains the ion-channel activity. In this dimer, the original carboxylic acids at C41 in AmB were converted to methyl ester and amide; thus the dimer is expected to have chemical and physical properties similar to those of AmB methyl ester (AME) rather than those of AmB. AME is known to be partitioned more preferentially to bilayer membranes than AmB.[33] To investigate the AmB–AmB interactions, selective observation of the channel assembly in lipid bilayers is essential, hence allowing us to focus on AME for a further study of channel assembles.

In this study, we prepared ^{13}C, ^{19}F-labeled C–N dimer (dimer **5**, Fig. 1), and carried out $^{13}C\{^{19}F\}$REDOR experiments, aiming to estimate the interatomic distance between AME and AME.

2. Materials and methods

AmB was purchased from Nacalai Tesque (Kyoto, Japan). Ergosterol was from Tokyo Kasei (Tokyo, Japan) and palmitoyloleoylphosphatidylcholine (POPC) was from Avanti Polar Lipid Inc. (Alabaster, AL). All other chemicals were obtained from standard venders. Fmoc-14-F AmB **2** was derivatized from AmB as reported previously.[34]

2.1. Preparation of ^{13}C-AME 3

^{13}C-AME **3** was prepared from AmB following a general procedure. Briefly, the amino-group was protected by FmocOSu, and then carboxyl-group was converted to ^{13}C-methyl ester using $^{13}CH_3I$. Finally, Fmoc-protection was removed by piperidine. Yellow powder; R_f 0–0.1 (2/1-$CHCl_3$/MeOH). ESI-MS m/z 961.3[$(M+Na)^+$; calcd for $C_{47}{}^{13}CH_{75}NNaO_{17}$: 961.5]

2.2. Preparation of AME dimer 5

To a solution of aldehyde **6**[35] (42 mg, 117 μmol) in DMF-*i*-PrOH were added ^{13}C-AME **3** (100 mg, 106 μmol) and $NaBH(OAc)_3$ (90 mg, 424 μmol). After being stirred for 30 min at room temperature, the solution was poured into diethyl ether, and the precipitate was filtered over Celite. The precipitate was washed with diethyl ether and extracted with $CHCl_3$-MeOH 5:3. The extract was purified by column chromatography on SiO_2 with $CHCl_3$-MeOH 10:1 to afford a yellow solid (69.0 mg, 51%). To a solution of the yellow solid (92 mg, 72 μmol) in DMSO-*i*-PrOH 3:1 (2 mL) was added piperidine (32 μL, 433 μmol). After being stirred for 30 min at room temperature, diethyl ether was added to form a yellow precipitate, which was filtered over Celite. The precipitate was washed with diethyl ether and extracted with $CHCl_3$-MeOH 5:3, yielding derivative **7** (72 mg, 95%), which was used without further purification. Yellow powder; R_f 0–0.1 (3/1-$CHCl_3$/MeOH). ESI-MS m/z 1053.3[$(M+H)^+$; calcd for $C_{52}{}^{13}CH_{86}N_3O_{18}$: 1053.59].

To a solution of Fmoc-14-F AmB **2** (12 mg, 10 μmol) in DMF (500 μl) were added diisopropylethylamine (5 μL, 30 μmol), and PyBOP (6 mg, 11 μmol). After being stirred for 1 h at room temperature, derivative **7** (11 mg, 10 μmol) was added to the solution. After being stirred for 23 h at room temperature, piperidine (6 μL, 60 μmol) was added. After being stirred for 1 h, diethyl ether was added to the solution to form a yellow precipitate. The precipitate was filtered over Celite, washed with diethyl ether and extracted with $CHCl_3$-MeOH 1:1. The extract was purified by HPLC to afford dimer **5** (1.8 mg, 9% HPLC isolation). HPLC conditions: column, COSMOSIL $5C_{18}$-AR-II Φ 20 × 250 mm, flow rate, 4.0 mL/min, mobile phase, linear gradient of MeOH and 5 mM ammonium acetate (pH 5.3) from 70:30 to 100:0 for 30 min, retention time, 37 min. Yellow powder; R_f 0–0.1 (3/1-$CHCl_3$/MeOH). ^1H NMR (500 MHz, DMSO-d_6) δ: 8.41 (1H, s), 7.79 (1H, s), 6.62–5.95 (41H, m), 5.54–5.40 (3H, m), 5.24–5.15 (3H, m), 4.35–3.99 (17H, m), 3.16–3.09 (10H, m), 2.95–2.84 (6H, m), 2.35–2.06 (19H, m), 1.42–1.22 (25H, m), 1.15–1.07 (17H, m), 1.02 (6H, d, J = 7.7 Hz), 0.90 (6H, d, J = 6.6 Hz). ^{13}C NMR (125 MHz, DMSO-d_6) δ: 51.99. ^{19}F NMR (470 MHz, DMSO-d_6) δ: −205.5 (dd, J = 32.3, 52.1 Hz). ESI-MS m/z 1999.5 [$(M+Na)^+$; calcd for $C_{99}{}^{13}CH_{155}FN_4NaO_{34}$: 1999.0].

2.3. Determination of hemolytic activity

Freshly collected human blood was centrifuged for 5 min at 1000*g*, and separated erythrocytes were washed twice by suspending in PBS buffer (pH 7.4). Sedimented erythrocytes were then resuspended with PBS to 100-fold volume of the original blood. Gradually diluted drug solutions (DMSO solution, 4 μL) were added

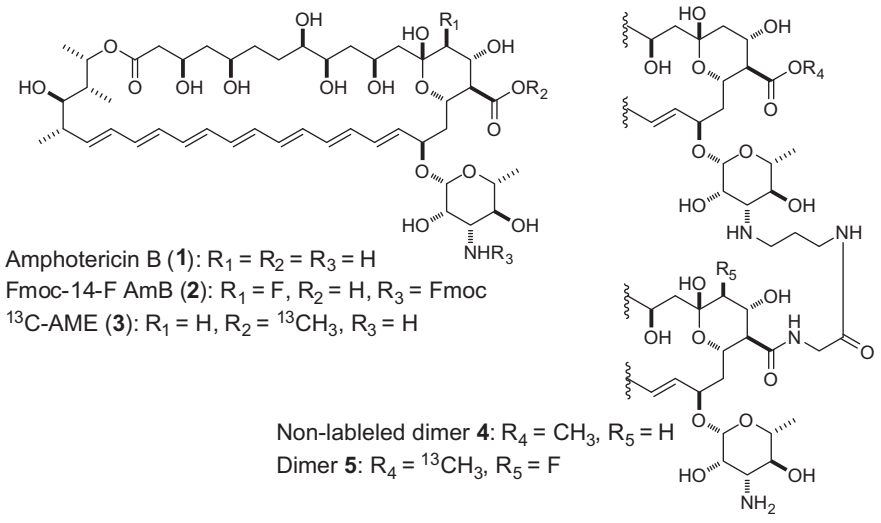

Figure 1. Structures of AmB **1**, ^{19}F- and ^{13}C-lableled AmBs, and dimers **4**, **5**.

to the erythrocyte suspensions (196 μL), and the suspensions were incubated with gently shaking at 38 °C. After 18 h, the suspensions were spun and the absorbance of the supernatant was determined at 450 nm by micro-plate reader (Molecular Devices). For a positive control, water was used instead of PBS buffer. As a negative control, 4 μL of DMSO was added instead of sample solution. From dose-response curves, the dosage that led to 50% hemolysis (EC_{50}) was determined.

2.4. Antifungal assay

Aspergillus niger was cultured in a GP liquid medium (2% glucose, 0.2% yeast extract, 0.5% polypeptone, 0.05% $MgSO_4$, and 0.1% KH_2PO_4) at 25 °C for 2 days. An aliquot of the broth was then spread onto a GP agar plate. The drugs dissolved in DMSO were spotted on paper disks of 8 mm in diameter. As a control, a disk containing only DMSO was also prepared. These paper disks were then placed on an agar plate containing *A. niger* mycelia. After cultivating at 25 °C for 50 h, the diameter of the inhibitory zone on each paper disk was measured.

2.5. Preparation of multilamellar vesicles

Dimer **5** (1.8 mg, 900 nmol), ergosterol (357 μg, 900 nmol), and POPC (6.2 mg, 8.1 μmol) were dissolved in $CHCl_3$/MeOH, and the solvent was evaporated to afford a thin film. After left in vacuo for 8 h, the membrane was hydrated with 8.4 μL of 10 mM HEPES buffer (pH 7.0) and 500 μL of H_2O and dispersed by vortexing and sonication. Then the lipid suspension was freeze-thawed five times to produce large vesicles. The suspension was lyophilized, rehydrated with D_2O (8.4 μL), and packed into a glass tube. The glass tube was sealed with epoxy glue and inserted into a φ 5 mm MAS rotor.

2.6. Solid-state NMR measurements

All solid-state NMR spectra were recorded on a CMX300 (Chemagnetics) spectrometer at 75 MHz ^{13}C resonance frequency with the MAS frequency of 5000 ± 2 Hz. The temperature controlling air was maintained at 30 ± 1 °C. The spectral width was 30 kHz. Typically, the π/2 pulse width for ^{1}H was 5 μs, and the π pulse widths for ^{13}C and ^{19}F were 11.0 and 10.3 μs, respectively. The contact times for cross-polarization transfer were set to be 1.5 ms for $^{13}C\{^{19}F\}$REDOR. The REDOR spectra were acquired with a recycle delay of 2 s under TPPM ^{1}H-decoupling[36] with field strength of 65.8 kHz, and xy-8 phase cycling[37] was used for ^{19}F.

3. Results and discussion

3.1. Preparation of dimer 5 and biological activity assays

Preparation of AME dimer **5** was shown in Scheme 1. Basically we followed our previous protocol by which non-fluorinated homologue of dimer **5** was prepared.[32] Briefly, aldehyde **6**[35] was coupled with ^{13}C-AME by reductive amino alkylation to give **7**, which was then coupled with *N*-Fmoc protected 14-F AmB. Removal of the Fmoc group, followed by HPLC purification, furnished dimer **5**.

Then biological activities of the dimer **5** were evaluated by hemolytic and antifungal assays to estimate the effect of fluorination since its non-fluorinated homologue **4** showed the comparable membrane activity to that of AmB. The results were summarized in Table 1. The hemolytic activity of dimer **5** was 6–7 times weaker than that of AmB or non-fluorinated dimer **4**.[32] Therefore, the fluorination somewhat attenuated the hemolytic activity. However, the hemolytic activity of dimer **5** is still potent, which is roughly

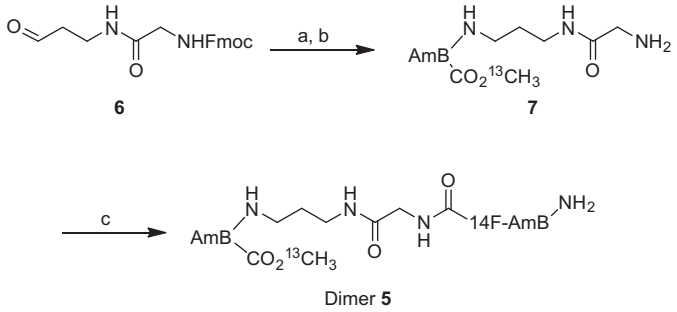

Scheme 1. (a) ^{13}C-AME **3**, $NaHB(OAc)_3$, DMF/*i*-PrOH, rt, 30 min, 51%; (b) piperidine, DMSO/*i*-PrOH, rt, 3 min, 95%; (c) Fmoc-14-F AmB **2**, PyBOP, DIPEA, DMF, rt, 23 h, then piperidine, rt, 1 h, 9%.

Table 1
Biological activity of AmB **1** and dimer **5**

	AmB **1**	dimer **5**
Hemolytic activity, EC_{50} [a] (μM)	2.0	13
Antifungal activity[b] (μg)	10	50

[a] Against 1% human erythrocytes.
[b] The minimal amount of a sample on a paper disk that shows inhibitory zone on the culture of *Aspergillus niger*.

comparable with that of AME.[38] The anti-fungal activity of **5**, albeit less efficacious than AmB, was similar to those of non-labeled dimer and other dimers.[29,32] The reduction of antibiotic activity of dimers may be accounted for by their less penetrability through fungal cell wall.

3.2. UV spectra measurement

For further confirming the formation of membrane-bound molecular assemblies of dimer in lipid bilayers, we recorded the UV spectra of non-labeled dimer **4** in ergosterol-containing POPC membrane, and compared them with those of AmB and AME. It is well known that absorption maxima at 414, 389 and 368 nm are characteristic of a monomeric form of AmB, and 354 nm is due to a molecular assembly.[7] As shown in Figure 2, the absorption maxima of the dimer, albeit higher intensity and small red shift of the peak at 415 nm, are very similar to those of AME. Upon comparison with AmB, the dimer showed a higher absorption at

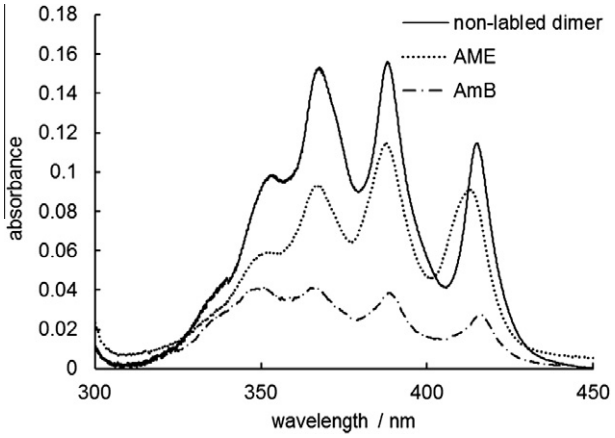

Figure 2. UV spectra of dimer **4** and AME in POPC membrane at the molar ratio of 0.005 and 0.01, respectively. The molar ratio of POPC/ergosterol was 9:1. The concentration of dimer and AME were 0.84 μM and 1.67 μM, respectively.

415 nm and a lower relative intensity of the peaks at 350 nm and 415 nm, both of which indicate that the dimer predominantly takes a non-aggregated form in lipid bilayers, although an aggregated form coexists.

3.3. Solid state NMR experiments

Next, we carried out the solid-state NMR measurements of dimer **5** in hydrated PC membrane. For sample preparation, dimer **5** was mixed in ergosterol-containing POPC membrane. Figure 3 showed non-irradiated (full-echo) (S_0) and ^{19}F-irradiated (S) spectra of ^{13}C{^{19}F}REDOR experiments. In the S_0 spectrum, a sharp signal at 54 ppm due to ^{13}C methyl ester was observed, which was significantly dephased by ^{19}F-irradiation as seen in the S spectrum. This unambiguously demonstrated the close vicinity between the fluorine atom and the methyl ester moiety of the dimer. To estimate the ^{19}F/^{13}C distance, the REDOR dephasing values ($\Delta S/S_0$) were plotted at various dephasing times (Fig. 4).

Generally, dipolar coupling constants depend on not only interatomic distance but also the orientation of dipolar tensor and molecular motion. We previously reported that AmB assemblies are mostly immobilized even in the hydrated membrane,[21] indicating that the dipolar coupling constants directly reflect the interatomic distance. The obtained dephasing effect was once saturated at around 20 ms (Fig. 4), clearly indicating the presence of relatively short ^{13}C/^{19}F distance. Additionally, the dephasing ratio increases again after 25 ms and keeps increasing up to 64 ms, which suggests that a longer ^{13}C/^{19}F distance (probably over 11 Å) also contributes to the REDOR dephasing. Considering the length of the crosslinker (ca 10 Å), the extended conformation of the dimer should lead to the ^{13}C/^{19}F distance of 11 Å or more. This means that the REDOR dephasing due to the distant ^{13}C/^{19}F pair is unlikely to be derived from an ion channel assembly. The best fit curve was obtained under the assumption of dual components in the dephasing effects; one is 6.9 Å distance that comprises 23% (Fig. 4, dashed line), and the other is 14 Å distance accounting for 77% (Fig. 4, dotted line). To confirm the coexistence of these two components, we examined the chemical shift distribution and relaxation time (Fig. S5, supporting information). However, we could not find evidence for the presence of the two components. This may be because the two components (23% and 77%) have similar chemical shifts and relaxation properties.

The above discussion is based on the assumption that the dimer is immobilized in the membrane as is the case of monomeric AmB;

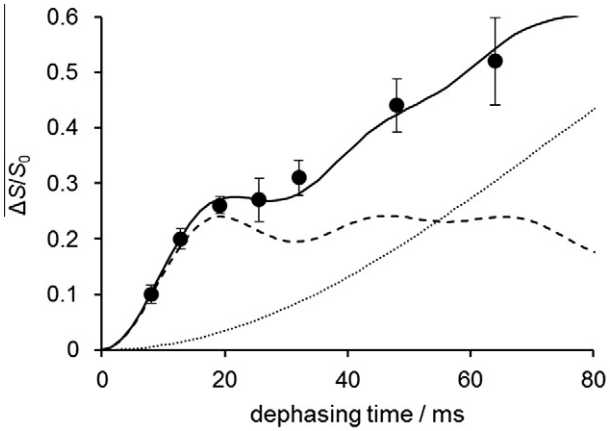

Figure 4. Experimental ^{13}C{^{19}F}REDOR dephasing values ($\Delta S/S_0$) for ^{13}C-metyl ester at 55 ppm (●), and simulation curves. Best fit curve (–) was obtained as assuming two components; 23% of 6.9 Å (dashed line) and 77 % of 14 Å (dotted line). See text for details.

however, it might be also possible to account for the biphasic feature of the REDOR dephasing curve by a slow motion of the dimer on the time scale of subseconds. To rule out this possibility, we measured REDOR at lower temperature (−2 °C), and found that the results are not different from the data in Figure 4 (Fig. S4, supporting information), thus confirming the immobilization of the dimer at the experimental temperatures.

Interestingly, the presence of two components shown in the REDOR experiment is consistent with the coexistence of aggregated and non-aggregated forms of the dimer in the UV spectra (Fig. 2). Considering the predominance of the non-aggregated form upon the UV measurements, the two components of 23% (shorter distance) and 77% (longer distance) are likely to correspond to the aggregated and non-aggregated forms, respectively.

It was recently reported that a single ion channel consists of six AmB molecules,[31] and the channel pore diameter is about 7.4 Å.[39] Based on these assumptions, the ^{13}C/^{19}F distance between AmB molecules is estimated to be 6–8 Å. Thus, the shorter component in the REDOR experiment is presumably due to the ^{13}C/^{19}F pair in an ion channel assembly. We previously calculated the lowest energy conformation of non-labeled dimer **4** in vacuo,[32] in which the poly-hydroxyl region of AmB portions comes face to face with each other so as to form multiple intramolecular hydrogen bonds.

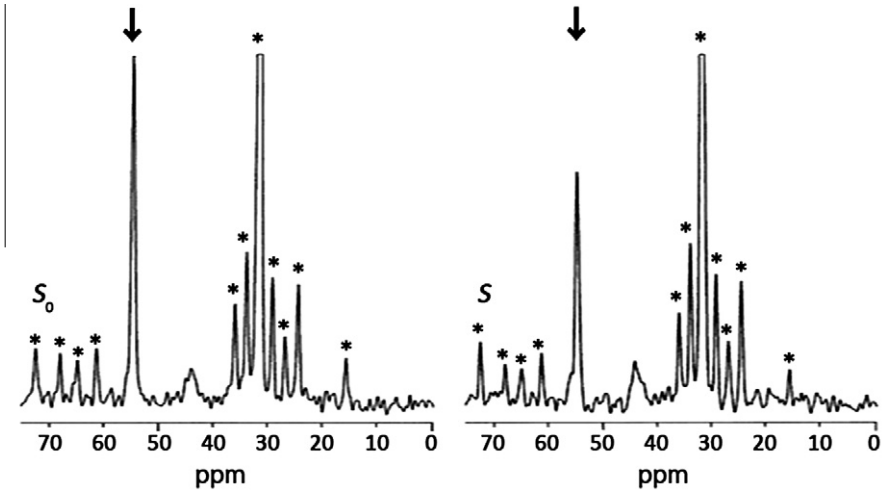

Figure 3. ^{13}C{^{19}F}REDOR spectra of non-irradiated (full-echo) (S_0) and ^{19}F-irradiated experiments (S) for dimer **5** at the ratio of **5**/ergosterol/POPC (1/1/9); hydrated POPC bilayers were prepared in 10 mM HEPES/D_2O (50% wt) at pH 7.0. The data were obtained after ^{19}F dephasing period of 160 rotor cycles (32 ms) at 38 °C with 23728 scans for each experiment. Arrows depict the ^{13}C-metyl ester signal. *^{13}C signals are those of POPC acyl chains.

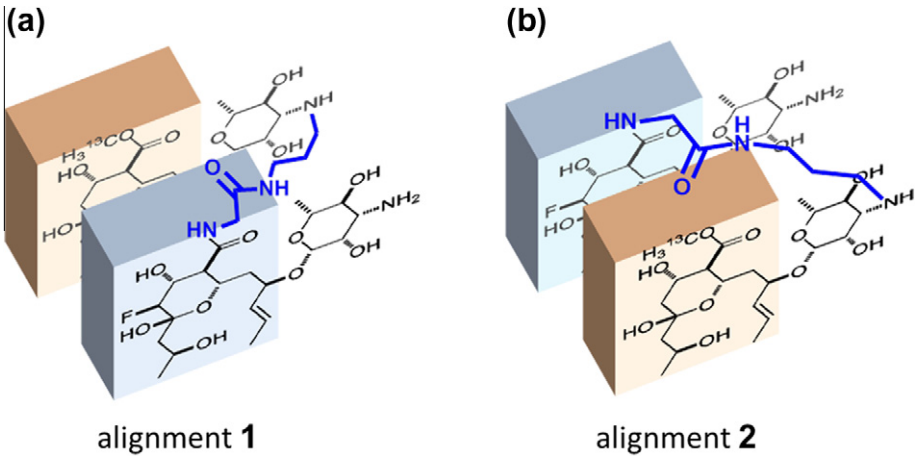

Figure 5. Possible arrangements of dimer **5**. (a) Front side of ^{13}C-AME moiety faces back side of F-14 AME moiety. (b) Front side of 14-F AME moiety faces back side of ^{13}C-AME moiety.

This face-to-face conformation is thought to be suitable for membrane penetration rather than channel formation upon membrane binding of the dimer. However, if dimer **5** takes a similar conformation, ^{13}C/^{19}F intramolecular distance should be 9 Å, which is much longer than the distance derived from the dephasing curve (6.9 Å). Therefore, the REDOR results suggest that dimer **5** takes different conformation from the calculated one, hence implying the presence of oligomeric AME units that may correspond to an ion channel assembly.

Figure 5 schematically depicts two possible arrangements of AME units in dimer **5**, in which a linker connects the inner side (a) and the outer side (b) of two AME units. Taking account of the length of the linker (ca 10 Å), alignment **1** is more reasonable because alignment **2** requires a longer linker (11–13 Å). Therefore, the ^{13}C/^{19}F distance of 6.9 Å can be derived from alignment **1** (Fig. 5a).

Although these models are based on an assumption that all the AME units in an assembly should be in the parallel orientation, there is a possibility that their direction is anti-parallel. If the dimer forms a barrel-stave-type of ion channel assemblies with the parallel orientation in membrane, the ^{13}C atom of methyl ester should come close to two ^{19}F atoms; one is an intramolecular ^{19}F atom and the other is that of the neighboring dimer. In that case, the ^{13}C/^{19}F REDOR curve should be simulated using F–C–F three-spin systems. Thus we simulated possible REDOR dephasing curves with 3 spin system for the 23% component which would reflect the channel structure, and with 2 spin system for the 77% component (11 Å) (detailed simulation data are given in Figs. S2 and S3, Supporting Information). However, all simulation curves saturated around 20 ms. Therefore differences in intermolecular ^{13}C/^{19}F distance and ^{19}F–^{13}C–^{19}F angle constraints do not greatly affect the intramolecular ^{13}C/^{19}F distance obtained from the two spin system (Fig. 4). This notion indicates that the evaluation of the intramolecular distances is less dependent on the presence or absence of ^{19}F atoms outside of the dimer. In other words, it would be difficult to obtain information on the orientation between adjacent dimers.

In the previous report,[25] we have estimated the AmB–AmB distance using monomeric ^{19}F- and ^{13}C-labeled AmBs (not AME) by the same method, and deduced the intermolecular distance to be 11–12 Å, which is significantly longer than the value (6.9 Å) in the present study. It may be partly caused by the effect of covalent linkage, which attracts AME units closer in the membrane assembly. Another possible explanation is that some of our previous assumptions upon estimating the intermolecular ^{13}C/^{19}F distance were inappropriate. Upon estimation,[25] we assumed that the parallel orientation exclusively occurred for AmB paring, which was reasonable for AmB units in a dimer but not necessarily for monomeric AmB molecules, because recent reports[31,40] suggested a possibility of anti-parallel orientation between AmBs in membrane. In addition, a short ^{13}C relaxation time and low ^{13}C-labeling rate of AmB in the previous study hampered the accurate measurements of the S/S_0 values for longer dephasing time over 32 ms; REDOR curve fitting for a shorter period could be the main cause for overestimation of the interatomic ^{13}C/^{19}F distance. Actually, the 14-F and C41 atoms in the previous report[25] seem to reside too apart to form a closely packed ion channel assembly. To re-examine the distance, REDOR experiments using monomeric 14-F AME and ^{13}C-AME are currently under way.

Meanwhile, it turned out to be difficult to extract the structural information of dimer **5** from the longer component (14 Å) of the REDOR dephasing. It was recently shown by a spectroscopic method[41,42] that AmB takes both perpendicular and parallel orientations with respect to the membrane surface; therefore, the longer component may reflect such parallel orientation, where the dimers lie on the membrane surface without extensive intermolecular interaction. This orientation is consistent with the UV spectrum of the dimer, which showed the significant absorption due to a non-aggregated form (Fig. 2), and therefore unlikely to be implicated in the ion channel assemblies.

In conclusion, to obtain more precise AME–AME distance, we prepared dimer **5** of ^{13}C and ^{19}F-label AMEs with an amide-type linker. Then the dimer was subjected to solid-state NMR measurements under hydrated bilayer membrane environments. Although 77% of dimer **5** stayed in a disassembled form, we could observe the ^{13}C/^{19}F REDOR dephasing effects from the remaining 23% of 'aggregated' dimers. The distance was successfully estimated to be 6.9 Å, which was a reasonable value for a closely packed assembly of AME.

Acknowledgments

This work is supported by Grants-in-Aid for Scientific Research (S) (No. 18101010), for Priority Area (A) (No. 16073211) and (B) (No. 17681027) from MEXT, Japan, and in part by JST, ERATO, 'lipid active structure project.'

Supplementary data

Supplementary data associated with this article can be found, in the online version, at http://dx.doi.org/10.1016/j.bmc.2012.08.016.

References and notes

1. Hartsel, S.; Bolard, J. *Trends Pharmacol. Sci.* **1996**, *17*, 445.
2. Lemke, A.; Kiderlen, A. F.; Kayser, O. *Appl. Microbiol. Biotechnol.* **2005**, *68*, 151.
3. De Kruijff, B.; Demel, R. A. *Biochim. Biophys. Acta* **1974**, *339*, 57.
4. Bolard, J. *Biochim. Biophys. Acta* **1986**, *864*, 257.
5. Kotler-Brajtburg, J. H.; Price, H. D.; Medoff, G.; Schlessinger, D.; Kobayashi, G. S. *Antimicrob. Agents Chemocher.* **1974**, *5*, 377.
6. Vertut-Croquin, A.; Bolard, J.; Chabbert, M.; Gary-Bobo, C. *Biochemistry* **1983**, *22*, 2939.
7. Baginski, M.; Resat, H.; McCammon, J. A. *Mol. Pharmacol.* **1997**, *52*, 560.
8. Baginski, M.; Resat, H.; Borowski, E. *Biochim. Biophys. Acta* **2002**, *1567*, 63.
9. Czub, J.; Baginski, M. *J. Phys. Chem. B* **2006**, *110*, 16743.
10. Fujii, G.; Chang, J. E.; Coley, T.; Steere, B. *Biochemistry* **1997**, *36*, 4959.
11. Cotero, B. V.; Rebeolledo-Antúnez, S.; Ortega-Blake, I. *Biochim. Biophys. Acta* **1998**, *1375*, 43.
12. Gagoś, M.; Koper, R.; Gruszecki, W. I. *Biochim. Biophys. Acta* **2001**, *1511*, 90.
13. Paquet, M. J.; Fournier, I.; Barwicz, J.; Tancrède, P.; Auger, M. *Chem. Phys. Lipids* **2002**, *119*, 1.
14. Dufourc, E. J.; Smith, I. C. P.; Jarrell, H. C. *Biochim. Biophys. Acta* **1984**, *778*, 435.
15. Soolovieva, S. E.; Olsufyeva, E. N.; Preobrazhenskaya, M. N. *Russ. Chem. Rev.* **2011**, *80*, 103.
16. Gray, K. C.; Palacios, D. S.; Dailey, I.; Endo, M. M.; Uno, B. E.; Wilcock, B. C.; Burke, M. D. *Proc. Natl. Acad. Sci. U.S.A.* **2012**, *109*, 2234.
17. Palacios, D. S.; Dailey, I.; Siebert, D. M.; Wilcock, B. C.; Burke, M. D. *Proc. Natl. Acad. Sci. U.S.A.* **2011**, *108*, 6733.
18. Matsumori, N.; Sawada, Y.; Murata, M. *J. Am. Chem. Soc.* **2005**, *127*, 10667.
19. Neumann, A.; Baginski, M.; Czub, J. *J. Am. Chem. Soc.* **2010**, *132*, 18266.
20. Croatt, M. P.; Carreira, E. M. *Org. Lett.* **2011**, *13*, 1390.
21. Matsumori, N.; Tahara, K.; Yamamoto, H.; Morooka, A.; Doi, M.; Oishi, T.; Murata, M. *J. Am. Chem. Soc.* **2009**, *131*, 11855.
22. Matsumori, N.; Kasai, Y.; Oishi, T.; Murata, M.; Nomura, K. *J. Am. Chem. Soc.* **2008**, *130*, 4757.
23. Gullion, T.; Schaefer, J. *Adv. Magn. Reson.* **1989**, *13*, 57.
24. Gullion, T.; Schaefer, J. *J. Magn. Reson.* **1989**, *81*, 196.
25. Umegawa, Y.; Matsumori, N.; Oishi, T.; Murata, M. *Biochemistry* **2008**, *47*, 13463.
26. Kasai, Y.; Matsumori, N.; Umegawa, Y.; Matsuoka, S.; Ueno, H.; Ikeuchi, H.; Oishi, T.; Murata, M. *Chem. Eur. J.* **2008**, *14*, 1178.
27. Umegawa, Y.; Nakagawa, Y.; Tahara, K.; Tuchikawa, H.; Matsumori, N.; Oishi, T.; Murata, M. *Biochemistry* **2012**, *51*, 83.
28. Matsumori, N.; Yamaji, N.; Matsuoka, S.; Oishi, T.; Murata, M. *J. Am. Chem. Soc.* **2002**, *124*, 4180.
29. Matsumori, N.; Masuda, R.; Murata, M. *Chem. Biodiver.* **2004**, *1*, 346.
30. Yamaji, N.; Matsumori, N.; Matsuoka, S.; Oishi, T.; Murata, M. *Org. Lett.* **2002**, *4*, 2087.
31. Hirano, M.; Takeuchi, Y.; Matsumori, N.; Murata, M.; Ide, T. *J. Membr. Biol.* **2011**, *240*, 159.
32. Umegawa, Y.; Matsumori, N.; Oishi, T.; Murata, M. *Tetrahedron Lett.* **2007**, *48*, 3393.
33. Readio, J. D.; Bittman, R. *Biochim. Biophys. Acta* **1982**, *685*, 219.
34. Matumori, N.; Umegawa, Y.; Oishi, T.; Murata, M. *Bioorg. Med. Chem. Lett.* **2005**, *15*, 3565.
35. Matsumori, N.; Sawada, Y.; Murata, M. *J. Am. Chem. Soc.* **2006**, *128*, 11977.
36. Bennett, A. E.; Rienstra, C. M.; Auger, M.; Lakshmi, K. V.; Griffin, R. G. *J. Chem. Phys.* **1995**, *103*, 6951.
37. Gullion, T.; Baker, D. B.; Conradi, M. S. *J. Magn. Reson.* **1990**, *89*, 479.
38. Chéron, M.; Cybulska, B.; Mazerski, J.; Grzybowska, J.; Czerwiński, A.; Borowski, E. *Biochem. Pharmacol.* **1988**, *37*, 827.
39. Katsu, T.; Okada, S.; Imamura, T.; Komagoe, K.; Masuda, K.; Inoue, T.; Nakao, S. *Anal. Sci.* **2008**, *24*, 1551.
40. Wasko, P.; Luchowski, R.; Tutaj, K.; Grudzinski, W.; Adamkiewicz, P.; Gruszecki, W. I. *Mol. Pharmaceutics* **2012**, *9*, 1511.
41. Gruszecki, W. I.; Gagoś, M.; Hereć, M. *J. Photochem. Photobiol. B: Biol.* **2003**, *69*, 49.
42. Hereć, M.; Islamov, A.; Kuklin, A.; Gagoś, M.; Gruszecki, W. I. *Chem. Phys. Lip.* **2007**, *147*, 78.